




Article

A GIS-Based Framework to Analyze the Behavior of Urban Greenery During Heatwaves Using Satellite Data

Barbara Cardone ¹, Ferdinando Di Martino ^{1,2,*}, Cristiano Mauriello ¹ and Vittorio Miraglia ¹

¹ Department of Architecture, University of Naples Federico II, Via Toledo 402, 80134 Napoli, Italy; b.cardone@unina.it (B.C.); cristiano.mauriello@unina.it (C.M.); vittorio.miraglia@unina.it (V.M.)

² Center for Interdepartmental Research “Alberto Calza Bini”, University of Naples Federico II, Via Toledo 402, 80134 Napoli, Italy

* Correspondence: fdimarti@unina.it; Tel.: +39-081-2538904

Abstract: This work proposes a new unsupervised method to evaluate the behavior of urban green areas in the presence of heatwave scenarios by analyzing three indices extracted from satellite data: the Normalized Difference Vegetation Index (NDVI), the Normalized Difference Moisture Index (NDMI), and Land Surface Temperature (LST). The aim of this research is to analyze the behavior of urban vegetation types during heatwaves through the analysis of these three indices. To evaluate how these indices characterize urban green areas during heatwaves, an unsupervised classification method of the three indices is proposed that uses the Elbow method to determine the optimal number of classes and the Jenks classification algorithm. Each class is assigned a Gaussian fuzzy set and the green urban areas are classified using zonal statistics operators. The membership degree of the corresponding fuzzy set is calculated to assess the reliability of the classification. Finally, for each type of greenery, the frequencies of types of green areas belonging to NDVI, NDMI, and LST classes are analyzed to evaluate their behavior during heatwaves. The framework was tested in an urban area consisting of the city of Naples (Italy). The results show that some types of greenery, such as deciduous forests and olive groves, are more efficient, in terms of health status and cooling effect, than other types of urban green areas during heatwaves; they are classified with NDVI and NDMI values of mainly High and Medium High, and maximum LST values of Medium Low. Conversely, uncultivated areas show critical behaviors during heatwaves; they are classified with maximum NDVI and NDMI values of Medium Low and maximum LST values of Medium High. The research results represent a support to urban planners and local municipalities in designing effective strategies and nature-based solutions to deal with heat waves in urban settlements.

Keywords: urban greenery; heatwave; GIS; Jenks classification method; Gaussian fuzzy set; NDVI; NDMI; LST



Citation: Cardone, B.; Di Martino, F.; Mauriello, C.; Miraglia, V. A GIS-Based Framework to Analyze the Behavior of Urban Greenery During Heatwaves Using Satellite Data. *ISPRS Int. J. Geo-Inf.* **2024**, *13*, 377. <https://doi.org/10.3390/ijgi13110377>

Academic Editor: Wolfgang Kainz

Received: 4 September 2024

Revised: 18 October 2024

Accepted: 29 October 2024

Published: 30 October 2024



Copyright: © 2024 by the authors. Published by MDPI on behalf of the International Society for Photogrammetry and Remote Sensing. Licensee MDPI, Basel, Switzerland. This article is an open access article distributed under the terms and conditions of the Creative Commons Attribution (CC BY) license (<https://creativecommons.org/licenses/by/4.0/>).

1. Introduction

The growing phenomenon of summer heat waves in urban settlements is producing continuous alerts in local administrations due to the risks to the health of the population, especially vulnerable groups and the chronically ill. Recent research has focused on assessing the current and future risks posed by heat wave scenarios in urban settlements. They have pointed out the increasing risks to the health of citizens over time, and the necessity of implementing mitigation strategies and adapting to the phenomenon [1–3].

The protection of the urban green ecosystem becomes an important action to address mitigating these risks and making cities more resilient to summer heat waves. In fact, many recent studies have highlighted that the risk of urban overheating can be mitigated by enhancing and protecting green infrastructures [4–9].

In [10], an analysis of urban heat islands detected with an accurate clustering method showed that in about 96% of the detected heat islands, the percentage of urban greening

is lower than the average value calculated for the entire urban settlement. Therefore, the prevention of the effects of heat waves in cities requires protecting urban green areas and enhancing their health and cooling potential.

The use of remote sensing and spatial modeling techniques in GIS-based environments can allow monitoring the health of urban green areas and help make decisions for their protection. Recent works propose GIS-based models for assessing the quality of urban greenery. In [11], a model applied for the assessment of urban greenery efficiency is implemented in a GIS-based framework. A deep learning model is encapsulated in a GIS-based framework in [12] to analyze urban greenery changes over time. GIS-based models implemented to evaluate citizens' perception of the efficiency of urban green infrastructures are proposed in [13,14].

Remote sensing techniques have been widely used to analyze the characteristics of urban green areas and to monitor their health status. A review of these techniques is given in [15]. In [16], six remote sensing indices extracted from the Sentinel-2 RS multispectral sensor with a spatial resolution of up to 10 m are used to monitor urban green spaces.

One of the best-known remote sensing indices used to evaluate the presence of living vegetation is the Normalized Difference Vegetation Index (NDVI). It is based on measurements of the reflectance of light in the red and near-infrared bands, as the photosynthetically active leaf region absorbs most of the red light of the electromagnetic spectrum and reflects near-infrared light. Conversely, dry and dead vegetation reflects more red light, absorbing more near-infrared light.

Recently, NDVI has been used in many studies to measure the health of urban green spaces [17–20]. One of the main advantages of NDVI is that it represents a non-destructive tool for monitoring the livability of vegetation as it does not require direct contact with it. Additionally, it can be employed to monitor large areas that are covered by the satellite. Finally, it allows for the constant monitoring of the vegetation state, enabling the analysis of seasonal and multiannual variations.

However, in extremely dense vegetation areas, NDVI may become saturated, making it difficult to distinguish further changes in vegetation vigor. Furthermore, NDVI values can be influenced by the presence of bare soil, particularly in areas with sparse vegetation.

Although the presence of clouds and atmospheric and soil characteristics can produce disturbing effects in the measurement, when the quantitative vegetation monitoring problem addressed does not require a high spatial accuracy, it is not necessary to carry out elaborate corrections of these perturbations in the calculation of NDVI.

To assess moisture levels and hydric stress in urban greenery, other authors combine NDVI with the Normalized Difference Moisture Index (NDMI) [21–24].

NDMI is an index used mainly to evaluate the presence and distribution of humidity in the soil or vegetation. It is based on the analysis of multispectral images acquired in near-infrared and shortwave-infrared reflectance by satellite sensors or aircraft. The shortwave-infrared band is sensitive to variations in aqueous content in the vegetation, whereas near-infrared reflectance is influenced by the concentration of dry matter in the foliage.

The use of this index is widespread in agriculture, forestry, hydrology, and environmental monitoring, for assessing vegetation health, soil water availability, and general environmental conditions. For instance, it can be employed to monitor drought, identify areas susceptible to forest fires, or analyze crop water stress.

Combined with the Land Surface Temperature (LST), the NDVI and NDMI indices can provide key information for analyzing the resilient effectiveness of urban green areas during heat waves, and monitoring their health status and cooling potential.

LST measures the radiative temperature of the land; it refers to the temperature of the surface of bare soils, or of built or natural roofs, and is obtained from the infrared brightness temperatures measured at two channels centered at 11 and 12 μm , respectively. LST provides a measure of the canopy temperature of a plant cover and can provide synthetic information on the thermal behavior of an urban green space. Mean annual LST anomalies are used in [25] to detect urban heat islands in the city of New Delhi, in India.

1.1. Gaps in Related Models

Recent studies carried out on urban settlements have shown the existence of a correlation between LST and NDVI [26,27] and LST and NDMI [28]. Research carried out in [29] on the urban area of Kathmandu Valley in central Nepal showed the presence of a negative relationship, both between LST and NDVI and between LST and NDMI, verifying that, compared to dense urban areas, LST decreases in the presence of rural and agricultural areas, in which there is a sharp increase in NDVI and NDMI values. Recently, experiments performed in the city of Hamburg, in Germany [23,30], showed that, in parks, clay soils showed an average LST that is approximately 2 °C higher than that in sand-dominated soils.

Analyses carried out in the city of Dhaka in Bangladesh, using historical data to determine the variations in LST, NDVI, and NDMI over the last thirty years, highlighted that the reduction over time of the vigilance coverage in the city of Dhaka has caused a significant reduction in vegetation cover, an increase in surface temperatures, and a reduction in soil humidity over the last three decades [31].

The main limitation of these models is that they require the use of numerous indices and different correction processes for atmospheric and soil effects, which limit their portability.

1.2. Objectives of This Research

The aim of this research is to propose a new unsupervised method to evaluate the resilience capacity of urban green areas in the presence of observed heatwaves, based on NDVI, NDMI, and LST.

The choice of these three indices is dictated by the fact that the presence of living vegetation, which presents low water stress, high plant cover, and low surface radiometric temperature during periods of heat waves, can characterize the urban green area with a high level of effective resilience. Since the aim of this study is to test a method for evaluating the resilient effectiveness of types of urban green areas during heatwaves, a high accuracy in the measurement of the three indices is not necessary. In fact, the proposed method uses zonal statistical processes for the classification of urban green areas based on average values determined for each of the three indices; it has the advantage of being computationally fast and does not require a high spatial accuracy of the measurements. This means laborious corrections of atmospheric and soil distorting effects can be avoided, and allows the use of additional measurement indices of specific characteristics of urban green areas.

To evaluate how these three indices characterize urban green areas during periods of heat waves, a reclassification of the data raster of each index is carried out. After acquiring the remote sensing multispectral bands, each index is classified separately by applying the Jenks natural breaks thematic classification method proposed in [32,33]; this technique has the advantage of clustering spatial data in such a way as to minimize the within-group variance and maximize the between-group variance [34]. The Elbow method is applied to set the number of classes.

The use of this classification method allows each thematic class to be assigned a Gaussian fuzzy set defined by setting the average value and the standard deviation of the class as parameters. Through zonal statistical processes, each public green urban area, displayed as a polygon on the map, is assigned to a thematic class considering the average of the values of the index assigned to the pixels covering the polygon; furthermore, the reliability of the classification is assessed, given by the degree of membership of the corresponding Gaussian fuzzy set.

Finally, an analysis of the characterization of types of urban green areas in periods of heat waves is carried out by determining how the frequencies of urban green areas of a specific type are distributed in the classes into which the domain of each index is partitioned.

1.3. Contributions of the Research

The main contributions of this work are as follows:

- It analyzes the behavior of urban green areas during periods of heatwaves, to determine the types of urban greenery of green areas that are least vulnerable to heatwaves,

and then, most suitable for mitigating the effects of heatwaves in urban settlements. This behavior is deduced starting from LST, NDMI, and NDVI measurements, which allow us to evaluate the thermal responses, the health, and the humidity level of urban greenery.

- To characterize urban green areas, an unsupervised method of classification of the three indices—NDVI, NDMI, and LST—was developed, which uses the Jenks algorithm; the Elbow method is used to determine the optimal number of classes. This approach has the advantage of not requiring subjective evaluations for the classification of the three indices.
- The use of the Jenks classification method allows each class to be associated with a Gaussian fuzzy set; the mean degree of membership of green areas of a type of urban greenery of the fuzzy set related to an NDVI, NDMI, or LST class can be interpreted as the reliability of the assignment of these urban green areas to this class.

The main advantage of our method is that it is computationally fast and portable. In fact, it does not require further processing to correct atmospheric and soil effects, and does not require the analysis of additional indices that measure specific characteristics of urban green areas, as it does not require high accuracy of the measurements. For this reason, the proposed method can become an easily usable tool to support the decision maker in the evaluation of the health status and response of urban green areas during heatwaves.

In Section 2, the architectural model of the framework is presented, the phases of the method are discussed in detail, and the area of study is presented. Section 3 shows and discusses the results obtained by executing our method on the area of study. The concluding discussions are given in Section 4.

2. Materials and Methods

The framework analyzes the behavior of urban greenery typologies during heatwaves by considering the raster data indices, NDVI, NDMI, and LST, determined by multispectral satellite images. The next paragraphs briefly synthesize the three indices and the calculus needed to obtain their measures, and describe in detail the proposed framework, the case study of the city of Naples (Italy), and the data used to test our method.

2.1. Base Concepts: The Calculus of the NDVI, NDMI, and LST Indices

NDVI is based on measurements of the reflectance of light in the red (RED) and near-infrared (NIR) bands, and is given by the formula:

$$\text{NDVI} = \frac{\text{NIR} - \text{RED}}{\text{NIR} + \text{RED}} \quad (1)$$

where the red wavelength is absorbed by the chlorophyll of the plant and the infrared radiation is reflected by the plant canopy.

NDVI varies between -1 and $+1$. Values close to $+1$ indicate dense and healthy vegetation; on the contrary, values close to 0 or negative values indicate a paucity of vegetation, bare ground, or other non-vegetated surfaces. Generally, negative values are recorded in impervious open spaces such as urban streets or squares.

NDMI compares the response of vegetation in two different bands of the electromagnetic spectrum, generally near-infrared (NIR) and shortwave-infrared reflectance (SWIR); it is given by the formula:

$$\text{NDMI} = \frac{\text{NIR} - \text{SWIR}}{\text{NIR} + \text{SWIR}} \quad (2)$$

NDMI varies between -1 and $+1$. Values close to $+1$ indicate dense and healthy vegetation without water stress; however, values close to -1 indicate typical bare soils with very sparse or no vegetal cover.

The process used to derive LST is more complex than those needed to derive the other two indices. The algorithm used to derive LST from the thermal infrared channels is the split-window algorithm. The split-window algorithm assesses the LST by removing

the effects of atmospheric disturbance using atmospheric absorption in the two adjacent thermal infrared channels centered at about 11 μm and 12 μm . The algorithm used to calculate LST from Landsat 8 Thermal Infrared Sensors is described in detail in [35,36].

2.2. The Proposed Framework

The framework is schematized in Figure 1.

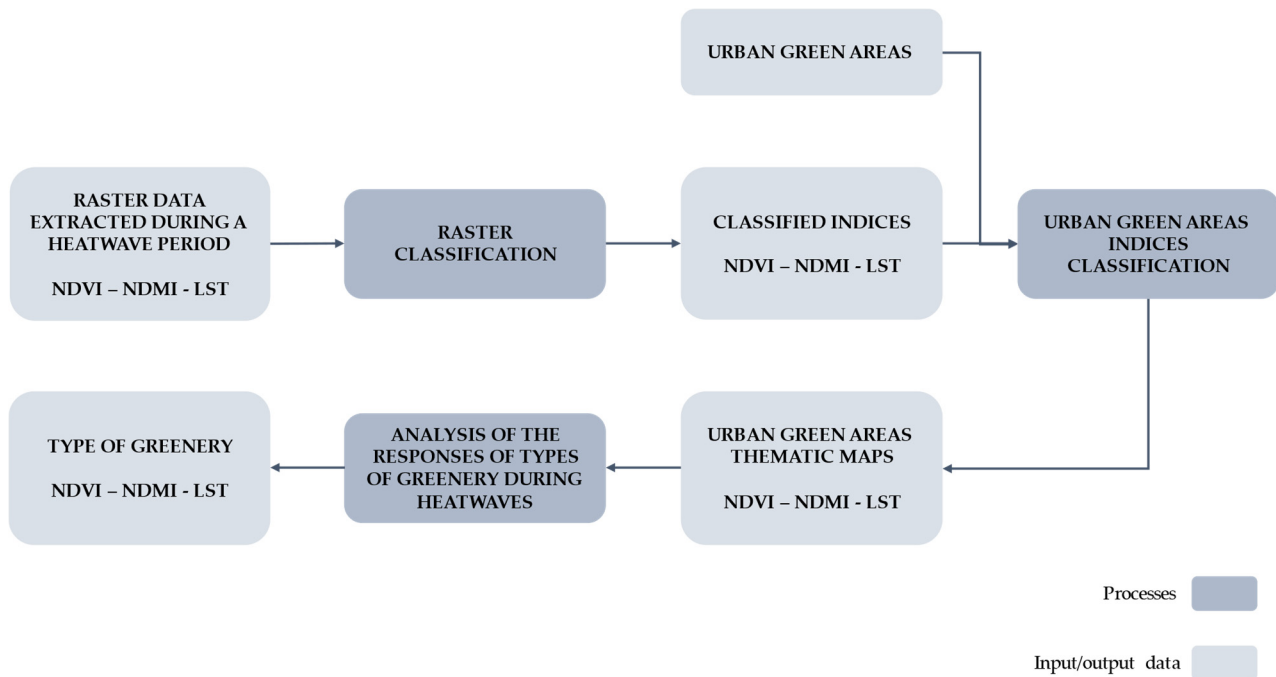


Figure 1. Schematic of the proposed framework, which schematizes the input data, consisting of satellite data raster, the spatial analysis processes, and the output data consisting of thematic maps and bar graphs of urban open spaces grouped by type of greenery for each index.

After extracting the raster data and giving the spatial distribution of the three indices during a heatwave, for each index, a raster classification process is performed. This process is implemented using the natural breaks thematic classification algorithm which, in partitioning the real interval corresponding to the index definition domain, determines the lower and upper bounds of the subset corresponding to each class (the breaks), so that the average standard deviation of the value of the pixel index assigned to each class is as small as possible.

We adopt the Elbow method to set the number of classes. The Elbow method is a heuristic approach applied in cluster analysis to set the optimal number of clusters, given by the number of clusters for which the curve of the trend of the quadratic sum of the distances of the data points from the centers of the clusters they belong to has an elbow; that is, for higher values of the number of clusters, the curve flattens.

Compared to other validity indices used for determining the optimal number of clusters, the Elbow method has the advantage of being fast; however, its main flaw is the ambiguity in determining the precise location of the curve elbow [37,38]. To overcome this limit, we propose to set the Elbow point equal to the value k of the number of classes for which the reduction in variance compared to that obtained with $k - 1$ classes is less than 25%.

Formally, let K be the number of classes in which the domain of the index is partitioned and let $\sigma_{K,i}^2$ be the variance of the index for the i th class, where $i = 1, 2, \dots, K$. The average variance obtained considering K classes is given by:

$$\overline{\sigma_K^2} = \frac{1}{K} \sum_{i=1}^K \sigma_{K,i}^2 \quad (3)$$

The reduction in variance with respect to the use of $K - 1$ classes is given by:

$$r\overline{\sigma_K^2} = \frac{\overline{\sigma_{K-1}^2} - \overline{\sigma_K^2}}{\overline{\sigma_{K-1}^2}} \quad (4)$$

The first value of the number of classes K for which $r\overline{\sigma_K^2}$ is less than 0.25 is selected as the Elbow point. The reason why the threshold is set to 0.25 is because when, as the number of classes K increases, and the reduction in variance $r\overline{\sigma_K^2}$ is reduced to 0.25, the curve has reached the plateau; therefore, for values of K greater than the Elbow point, the reduction in variance is negligible.

Figure 2 shows an example of the application of this approach for determining the optimal number of classes. The selected value for K is $K = 7$, where a value of $r\overline{\sigma_K^2}$ less than 0.25 is achieved.

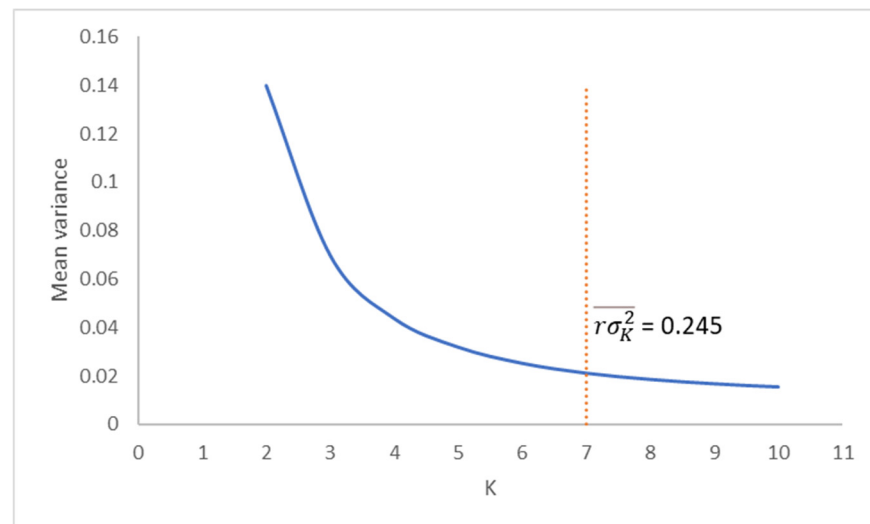


Figure 2. Example of Elbow point selection, for determining the optimal number of classes, with K value set to 7.

The result of the raster classification process is a raster dataset in which each pixel is assigned the identifier of the thematic class to which it belongs.

The Jenks natural breaks thematic classification method is used to build the K thematic classes. The Jenks algorithm is a thematic classification algorithm used to classify the domain of an index in K classes. It is an iterative clustering method that has the objective of partitioning the numerical interval of a measure into K classes, with K fixed a priori, in order to minimize the average standard deviation of each class and maximize the difference between the means of each class. It represents the optimal method of thematic classification since it is the one that statistically allows the optimization of the similarity of the elements of a class and the dissimilarity among the classes.

A label is assigned to each thematic class following the order of the class, and the term *Medium* is assigned to the central classes if K is odd, or the terms *Medium low* and *Medium high* are assigned if K is even. For example, if $K = 5$, the third class, which constitutes the central class, is assigned the label *Medium*, and the second and fourth classes, respectively, are assigned the labels *Medium low* and *Medium high*. Assuming $K = 6$, the third and fourth

classes are assigned the labels *Medium low* and *Medium high*, respectively, the labels *Low* and *High* are assigned to the second and fifth classes, and the labels *Very low* and *Very high* are assigned to the first and last classes.

In the next step, a classification of the urban green areas based on each index is performed, where the urban green areas in the area of study are given by polygons and each polygon is assigned the type of greenery. To carry out this classification, each thematic class into which the index domain has been partitioned is assigned a Gaussian fuzzy set, whose parameters are given by the average value and the standard deviation of the pixels belonging to the thematic class.

This process is performed by creating a Gaussian fuzzy partition of the domain of the index. This is a fuzzy partition of a numerical domain in K Gaussian fuzzy sets, where a Gaussian fuzzy set is a fuzzy number that assigns the two parameters of a Gaussian function, i.e., the mean and standard deviation. The choice of a Gaussian fuzzy partition is linked to the use of the Jenk thematic classification algorithm. In fact, each thematic class is assigned a fuzzy set of the fuzzy partition constituted by a Gaussian fuzzy number whose two parameters, the mean and standard deviation, are given by the mean and standard deviation of the class.

Formally, let μ_k and σ_k be, respectively, the mean and the standard deviation of the values of the pixels belonging to the k th thematic class, where $k = 1, \dots, K$. To this thematic class is assigned a Gaussian fuzzy cluster having the following membership function:

$$u_k(x) = e^{-\frac{1}{2}\left(\frac{x-\mu_k}{\sigma_k}\right)^2} \quad (5)$$

and having as a label the label of the thematic class.

For example, consider the following table, which shows the average and the standard deviation of the NDMI index for all the six thematic classes in which the domain is partitioned (Table 1).

Table 1. Example of partitioning of NDMI in six thematic classes.

| Thematic Class | Average | Standard Deviation |
|----------------|---------|--------------------|
| Very low | −0.48 | 0.06 |
| Low | −0.33 | 0.08 |
| Medium low | −0.11 | 0.08 |
| Medium high | 0.07 | 0.09 |
| High | 0.19 | 0.06 |
| Very high | 0.34 | 0.05 |

By assigning a fuzzy set to each thematic class, the following Gaussian fuzzy sets are obtained (Figure 3).

Using a zonal statistics process, to each polygon representing an urban green area, a value of the index given by the average of the values of the pixels covering this polygon is attributed; then, the label of the Gaussian fuzzy set to whom the polygon belongs, having the highest membership degree, is assigned to this polygon.

For example, if the average of the NDMI values of the pixels covering this polygon is 0.11, it is assigned the label *Medium high*, as it belongs to the Gaussian fuzzy set termed *Medium high* with the highest membership degree (0.92). This membership degree is interpreted as the uncertainty of this assignment.

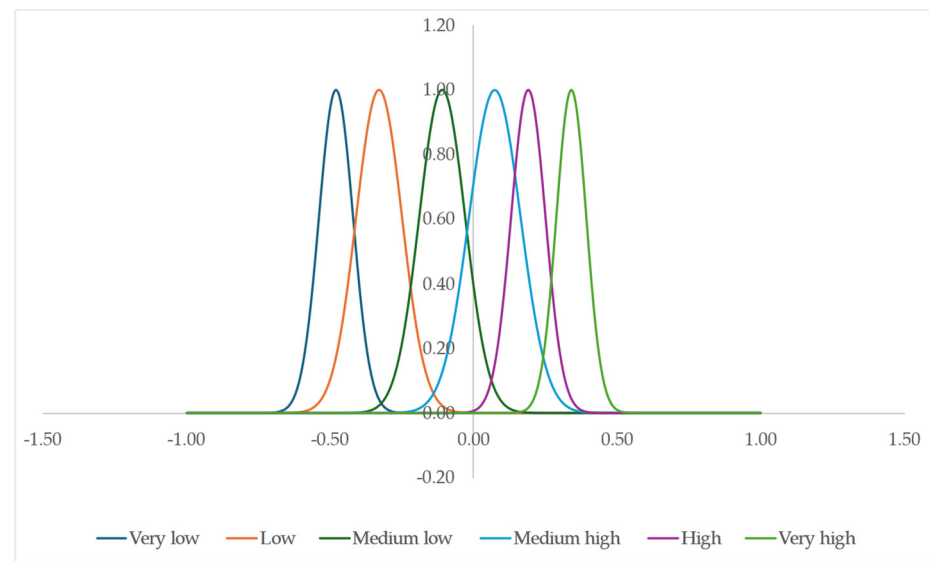


Figure 3. Gaussian fuzzy sets obtained by assigning a fuzzy set to each of the six thematic classes of the NDVI index in Table 1.

The outcomes of this step are three thematic maps in which the green areas are represented, respectively, by NDVI, NDMI, and LST classes. Each urban green area is assigned the labels of the NDVI, NDMI, and LST classes, the uncertainties of the assignment to each of the three classes, and the type of greenery.

In the last step, an analysis of the behavior of the different types of urban greenery during the heatwave is conducted. For each type of urban greenery and for each of the three indices, the frequencies of green areas falling into each of the thematic classes into which the index has been divided are determined. By comparing the frequency distributions of the three indices, it is possible to evaluate the behavior of the type of urban greenery during heatwaves. This analysis will allow us to detect the presence of types of urban greenery in which significant frequencies of urban areas belonging to specific NDMI, NDVI, and LST classes are recorded, and to verify whether, for these types of urban greenery, these classes relating to the three indices are correlated.

Furthermore, for each type of greenery and each class, a reliability is determined consisting of the average of the degrees of membership of the green areas of the corresponding Gaussian fuzzy set.

To clarify this process, the frequencies of vineyards belonging to six NDMI classes and the average membership degrees are shown as an example in Table 2.

Table 2. Example of frequency of vineyards distributed in the six NDMI classes.

| Thematic Class | Frequency | Mean Membership Degree |
|----------------|-----------|------------------------|
| Very low | 1 | 0.72 |
| Low | 16 | 0.65 |
| Medium low | 101 | 0.57 |
| Medium high | 192 | 0.57 |
| High | 161 | 0.53 |
| Very high | 34 | 0.60 |

The horizontal histogram in Figure 4 shows the distribution of frequencies obtained. The histogram highlights that approximately 70% of vineyards are classified with NDMI of High or Medium high; furthermore, over 76% of the vineyards are classified with NDMI of at least Medium high and a reliability of at least 67%.

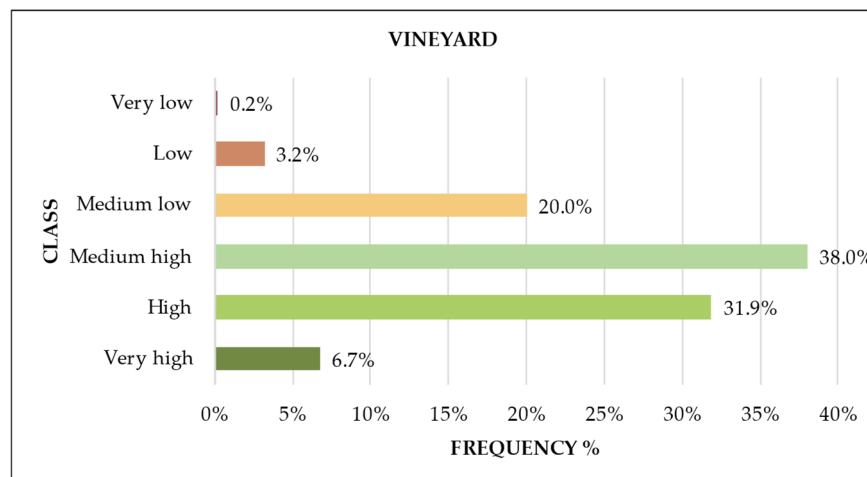


Figure 4. Histogram showing the frequencies of vineyards belonging to the six NDMI classes.

The mean membership degrees can be interpreted as the reliability of the assignment to a class of that frequency of urban greenery. In the example in Table 2, it is higher than 0.5, and can be considered acceptable, as the uncertainty in assigning vineyards to an NDMI class is negligible.

2.3. The Case Study

The city of Naples is a complex urban settlement with a high population density and building density.

The historic city center is the area with the greatest population and built density; it is characterized by a high percentage of impervious open spaces and few urban green spaces. The western and northwestern outskirts of the city are characterized by a greater extension of forest-type green spaces than the rest of the city. The eastern suburbs are predominantly industrial, with a high density of buildings along the coast and a predominance of impervious open spaces (Figure 5).

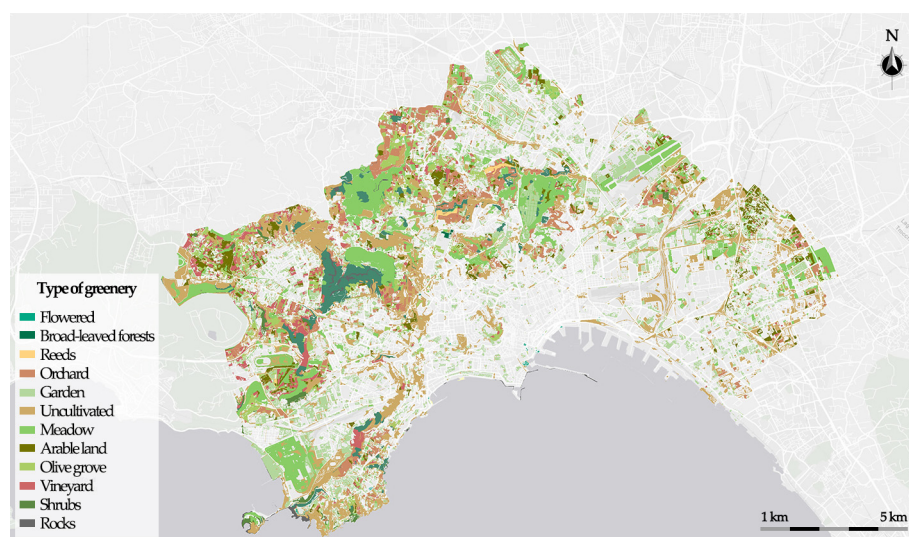


Figure 5. Thematic map showing the open spaces of the city of Naples (Italy) classified by types of greenery.

To test the framework, multispectral satellite data were acquired during a heatwave that occurred on 15 July 2023, where, following [3], a heatwave period refers to a time span of at least three consecutive days with a daily heat index higher than 32 °C. The climatic conditions of 15 July recorded the following values: maximum atmospheric temperature

of 32 °C, minimum atmospheric temperature of 23 °C, average humidity of 60%, and maximum humidity of 84%. The acquisition of these data was necessary for the creation of the raster data of the NDVI, NDMI, and LST indices.

In addition, the latest topographical base at scale 1:5000 provided by the Campania Region and updated to the year 2023 was used to extract all the green areas of the city as polygonal features. Table 3 shows the spatial and satellite resolution information.

Table 3. Satellite and spatial resolution of the three indices acquired on 15 July 2023.

| Index | Satellite/Bands | Resolution |
|-------|------------------------------|-----------------|
| NDVI | RapidEye bands RED and NIR | 7 m × 7 m |
| NDMI | Sentinel-2 bands B08 and B11 | 14.8 m × 14.8 m |
| LST | Landsat 8 band 10 | 30 m × 30 m |

The urban green areas are extracted as polygons from the regional topographic database at 1:5000 scale. Table 4 shows the number of polygons extracted for each type of greenery.

Table 4. Types of urban green areas extracted from the topographic database.

| Type of Greenery | Number of Polygons |
|------------------------------------|--------------------|
| Flowered | 142 |
| Predominantly broad-leaved forests | 209 |
| Reeds | 29 |
| Orchard | 532 |
| Garden | 4247 |
| Uncultivated | 4404 |
| Meadow | 611 |
| Arable land | 784 |
| Olive grove | 313 |
| Vineyard | 505 |
| Shrubs | 40 |
| Rocks | 46 |

The framework was implemented using the GIS platform ESRI ArcGIS Pro; the code was generated in the Python environment using the ESRI Python library.

In the next section, the results obtained are presented and discussed.

3. Results and Discussion

The proposed method is executed to classify, for each index, the urban green areas of the city of Naples. Section 3.1 shows the results obtained; a discussion of these results, including an analysis of the behavior of the types of greenery during heatwaves, is included in Section 3.2.

3.1. Outcomes Obtained

After creating the three-raster data for NDVI, NDMI, and LST, starting from the multiband satellite data taken on 15 July 2023, each index was treated separately in a reclassification process in which the Jenks thematic classification method was used for partitioning into classes. To determine the optimal number of classes, the Elbow method was used, by analyzing the trend of the average variance value as the number of classes varied.

The optimal number of classes is 6 for NDMI and 7 for NDVI and LST. Each thematic class is assigned a Gaussian fuzzy set where the parameter mean and standard deviation are given by the mean and standard deviation of the corresponding thematic class.

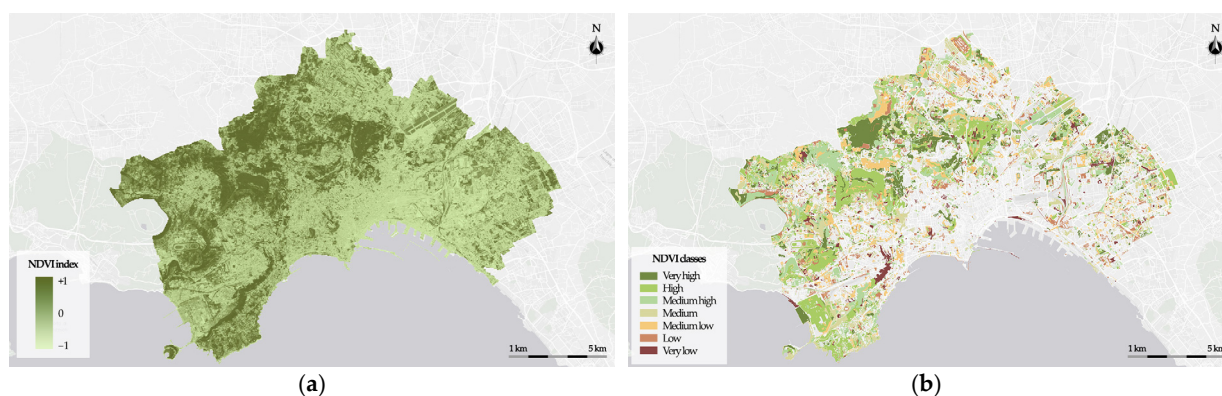
Table 5 shows, for each index, the label, mean, and standard deviation of the thematic classes.

Table 5. Label, mean, and standard deviation of the classes in which are partitioned the domains of NDVI, NDMI, and LST.

| Index | Label | Mean | Standard Deviation |
|-------|-------------|-------|--------------------|
| NDVI | Very low | 0.15 | 0.04 |
| | Low | 0.25 | 0.03 |
| | Medium low | 0.35 | 0.03 |
| | Medium | 0.47 | 0.04 |
| | Medium high | 0.60 | 0.04 |
| | High | 0.74 | 0.04 |
| NDMI | Very low | −0.25 | 0.06 |
| | Low | −0.13 | 0.03 |
| | Medium low | −0.03 | 0.03 |
| | Medium high | 0.07 | 0.03 |
| | High | 0.20 | 0.04 |
| | Very high | 0.36 | 0.05 |
| LST | Very low | 22.09 | 0.83 |
| | Low | 24.21 | 0.55 |
| | Medium low | 25.97 | 0.48 |
| | Medium | 27.56 | 0.42 |
| | Medium high | 28.91 | 0.38 |
| | High | 30.24 | 0.39 |
| | Very high | 31.63 | 0.62 |

The polygonal spatial dataset of the urban green areas was created by extracting from the topographical database and merging all the vector themes corresponding to types of urban green areas. Then, a zonal statistics method was implemented in the GIS platform to calculate statistics on cell values of the NDVI, NDMI, and LST raster within each urban green area. For each urban area, the mean value of NDVI, NDMI, and LST is calculated; then, the urban green area is assigned to the class corresponding to the Gaussian fuzzy set to which it belongs having the greatest membership degree.

Figures 6–8 show, respectively, for NDVI, NDMI, and LST, the map with the spatial distribution of the index and the thematic map of the urban green areas with the partitioning of the index domain into thematic classes.

**Figure 6.** The NDVI index thematic map (a) is compared with the greenery NDVI thematic map (b).

Comparison between the NDVI, NDMI, and LST thematic maps and the correspondent greenery thematic map highlights that, in the presence of urban green areas, the NDVI and NDMI values are higher than those in areas with high building density. On the contrary, the LST values in urban green areas are lower than those recorded in areas with high building density.

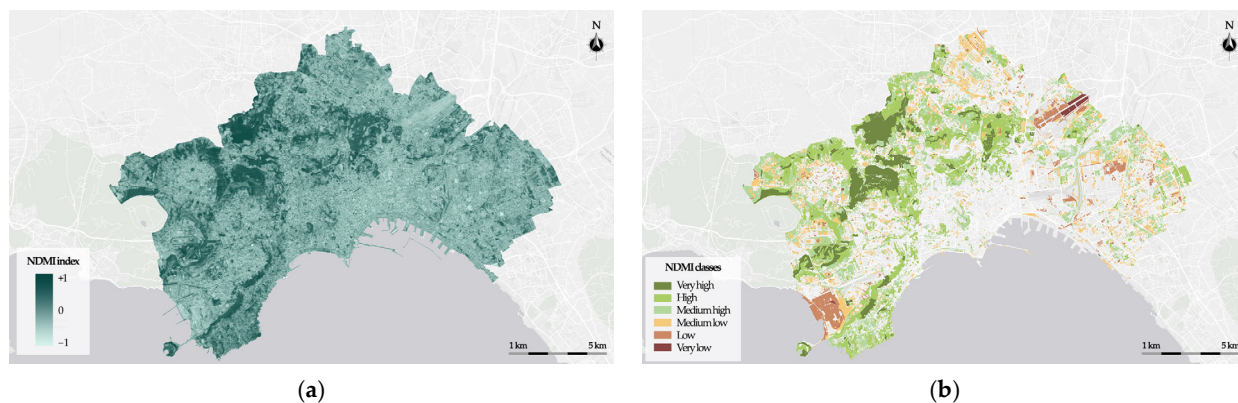


Figure 7. The NDMI index thematic map (a) is compared with the greenery NDMI thematic map (b).

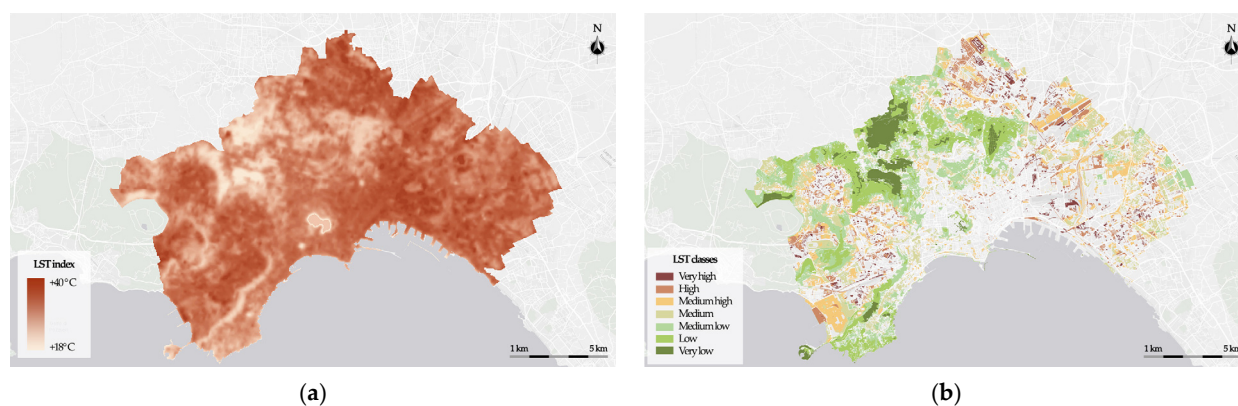


Figure 8. The LST Index thematic map (a) is compared with the greenery LST thematic map (b).

To carry out an analysis of the behavior of each type of greenery, for each type of greenery the frequencies of green areas belonging to the NDVI, NDMI, and LST classes are calculated. Tables 6–8 show, for each type of greenery, the frequencies of urban green areas belonging to each class of NDVI, NDMI, and LST, respectively.

Table 6. Frequency distribution of types of urban greenery belonging to the NDVI classes.

| Type of Greenery | Class | | | | | | |
|------------------------------------|----------|--------|------------|--------|-------------|--------|-----------|
| | Very Low | Low | Medium Low | Medium | Medium High | High | Very High |
| Flowered | 11.97% | 17.61% | 14.08% | 20.42% | 21.83% | 13.38% | 0.70% |
| Predominantly broad-leaved forests | 0.00% | 0.96% | 7.66% | 9.57% | 17.22% | 23.92% | 40.67% |
| Reeds | 0.00% | 0.00% | 3.45% | 24.14% | 17.24% | 41.38% | 13.79% |
| Orchard | 2.07% | 4.32% | 13.16% | 20.30% | 24.81% | 21.99% | 13.35% |
| Garden | 7.28% | 19.00% | 23.00% | 19.73% | 13.85% | 10.03% | 7.11% |
| Uncultivated | 6.38% | 16.39% | 19.50% | 18.23% | 16.33% | 13.44% | 9.72% |
| Meadow | 2.78% | 10.31% | 19.31% | 22.91% | 22.09% | 15.06% | 7.53% |
| Arable land | 3.06% | 7.02% | 15.69% | 20.28% | 19.52% | 18.49% | 15.94% |
| Olive grove | 0.96% | 2.88% | 12.78% | 19.49% | 23.96% | 29.39% | 10.54% |
| Vineyard | 0.73% | 2.38% | 10.26% | 18.68% | 23.81% | 24.91% | 19.23% |
| Shrubs | 0.00% | 0.00% | 12.50% | 12.50% | 32.50% | 27.50% | 15.00% |
| Rocks | 15.22% | 15.22% | 26.09% | 19.57% | 8.70% | 6.52% | 8.70% |

Table 7. Frequency distribution of types of urban greenery belonging to the NDMI classes.

| Type of Greenery | Class | | | | | |
|------------------------------------|----------|--------|------------|-------------|--------|-----------|
| | Very Low | Low | Medium Low | Medium High | High | Very High |
| Flowered | 0.70% | 4.93% | 33.10% | 42.25% | 17.61% | 1.41% |
| Predominantly broad-leaved forests | 0.00% | 2.39% | 12.44% | 21.05% | 35.41% | 28.71% |
| Reeds | 0.00% | 0.00% | 6.90% | 6.90% | 44.83% | 41.38% |
| Orchard | 0.38% | 4.32% | 13.16% | 37.97% | 36.84% | 7.33% |
| Garden | 0.82% | 13.40% | 40.24% | 33.60% | 9.65% | 2.28% |
| Uncultivated | 2.07% | 14.85% | 34.85% | 31.20% | 14.17% | 2.86% |
| Meadow | 1.15% | 9.49% | 28.97% | 33.88% | 21.28% | 5.24% |
| Arable land | 0.38% | 8.04% | 24.36% | 38.52% | 22.70% | 5.99% |
| Olive grove | 0.32% | 1.92% | 14.38% | 42.17% | 35.46% | 5.75% |
| Vineyard | 0.18% | 3.11% | 21.43% | 43.41% | 27.11% | 4.76% |
| Shrubs | 0.00% | 0.00% | 5.00% | 20.00% | 57.50% | 17.50% |
| Rocks | 0.00% | 8.70% | 32.61% | 19.57% | 21.74% | 17.39% |

Table 8. Frequency distribution of types of urban greenery belonging to the LST classes.

| Type of Greenery | Class | | | | | | |
|------------------------------------|----------|--------|------------|--------|-------------|--------|-----------|
| | Very Low | Low | Medium Low | Medium | Medium High | High | Very High |
| Flowered | 0.70% | 9.86% | 36.62% | 14.79% | 9.15% | 23.94% | 4.93% |
| Predominantly broad-leaved forests | 18.18% | 41.15% | 28.23% | 7.66% | 4.78% | 0.00% | 0.00% |
| Reeds | 17.24% | 37.93% | 31.03% | 6.90% | 6.90% | 0.00% | 0.00% |
| Orchard | 1.69% | 14.29% | 33.46% | 27.63% | 15.98% | 5.83% | 1.13% |
| Garden | 6.89% | 4.08% | 9.58% | 16.54% | 22.60% | 24.38% | 15.93% |
| Uncultivated | 1.59% | 6.61% | 14.51% | 23.43% | 25.50% | 20.80% | 7.56% |
| Meadow | 1.47% | 10.31% | 19.64% | 33.06% | 22.09% | 11.29% | 2.13% |
| Arable land | 2.42% | 13.90% | 26.40% | 34.06% | 17.35% | 5.10% | 0.77% |
| Olive grove | 0.32% | 16.93% | 35.78% | 30.67% | 13.10% | 3.19% | 0.00% |
| Vineyard | 2.01% | 5.86% | 13.37% | 25.64% | 33.15% | 17.22% | 2.75% |
| Shrubs | 12.50% | 27.50% | 40.00% | 15.00% | 5.00% | 0.00% | 0.00% |
| Rocks | 54.35% | 26.09% | 13.04% | 6.52% | 0.00% | 0.00% | 0.00% |

These results highlight the behavior of some types of greenery during heatwaves. Predominantly broad-leaved forests, reeds, and shrubs are mainly classified with maximum NDVI and NDMI of Medium high, and maximum LST of Medium Low.

Vineyards are mainly classified with maximum NDVI and NDMI of Medium high, but also with maximum LST of Medium high.

Gardens and uncultivated areas do not have high frequencies of belonging to specific NDVI and NDMI classes, although they are predominantly classified with LST between Medium and High.

Tables 9–11 show the reliability of the type of urban green area belonging to each class of the indices NDVI, NDMI, and LST, respectively, where the reliability is given by the mean membership degree of the corresponding Gaussian fuzzy set of the type of green area belonging to the class.

Table 9. Reliability distribution of types of urban greenery belonging to the NDVI classes.

| Type of Greenery | Class | | | | | | |
|------------------------------------|----------|-------|------------|--------|-------------|-------|-----------|
| | Very Low | Low | Medium Low | Medium | Medium High | High | Very High |
| Flowered | 0.864 | 0.798 | 0.748 | 0.643 | 0.642 | 0.768 | 0.655 |
| Predominantly broad-leaved forests | | 0.601 | 0.674 | 0.640 | 0.571 | 0.703 | 0.697 |
| Reeds | | | 0.572 | 0.769 | 0.708 | 0.671 | 0.679 |
| Orchard | 0.768 | 0.731 | 0.662 | 0.638 | 0.655 | 0.689 | 0.684 |
| Garden | 0.703 | 0.727 | 0.676 | 0.639 | 0.655 | 0.647 | 0.659 |
| Uncultivated | 0.727 | 0.694 | 0.670 | 0.633 | 0.645 | 0.649 | 0.712 |
| Meadow | 0.710 | 0.693 | 0.661 | 0.628 | 0.635 | 0.627 | 0.704 |
| Arable land | 0.725 | 0.680 | 0.666 | 0.610 | 0.672 | 0.637 | 0.670 |
| Olive grove | 0.564 | 0.790 | 0.627 | 0.661 | 0.662 | 0.639 | 0.650 |
| Vineyard | 0.610 | 0.766 | 0.680 | 0.685 | 0.681 | 0.649 | 0.704 |
| Shrubs | | | 0.680 | 0.728 | 0.610 | 0.555 | 0.666 |
| Rocks | 0.540 | 0.609 | 0.607 | 0.664 | 0.574 | 0.811 | 0.651 |

Table 10. Reliability distribution of types of urban greenery belonging to the NDMI classes.

| Type of Greenery | Class | | | | | | |
|------------------------------------|----------|-------|------------|--------|-------------|-------|-----------|
| | Very Low | Low | Medium Low | Medium | Medium High | High | Very High |
| Flowered | | 0.715 | 0.667 | 0.643 | 0.654 | 0.659 | |
| Predominantly broad-leaved forests | | | 0.633 | 0.587 | 0.602 | 0.725 | |
| Reeds | 0.576 | 0.682 | 0.689 | 0.705 | 0.683 | 0.634 | 0.576 |
| Orchard | 0.660 | 0.684 | 0.698 | 0.679 | 0.617 | 0.618 | 0.660 |
| Garden | 0.687 | 0.700 | 0.692 | 0.675 | 0.653 | 0.644 | 0.687 |
| Uncultivated | 0.574 | 0.733 | 0.728 | 0.665 | 0.655 | 0.650 | 0.574 |
| Meadow | 0.528 | 0.596 | 0.663 | 0.670 | 0.626 | 0.642 | 0.528 |
| Arable land | 0.991 | 0.688 | 0.684 | 0.694 | 0.677 | 0.677 | 0.991 |
| Olive grove | 0.759 | 0.608 | 0.677 | 0.697 | 0.681 | 0.656 | 0.759 |
| Vineyard | | | 0.678 | 0.672 | 0.718 | 0.622 | |
| Shrubs | 0.574 | 0.733 | 0.728 | 0.665 | 0.655 | 0.650 | 0.574 |
| Rocks | | 0.715 | 0.667 | 0.643 | 0.654 | 0.659 | |

Table 11. Reliability distribution of types of urban greenery belonging to the LST classes.

| Type of Greenery | Class | | | | | | |
|------------------------------------|----------|-------|------------|--------|-------------|-------|-----------|
| | Very Low | Low | Medium Low | Medium | Medium High | High | Very High |
| Flowered | 0.575 | 0.559 | 0.575 | 0.639 | 0.554 | 0.665 | 0.685 |
| Predominantly broad-leaved forests | | 0.725 | 0.685 | 0.633 | 0.677 | | |
| Reeds | | 0.644 | 0.692 | 0.551 | 0.848 | | |
| Orchard | 0.544 | 0.673 | 0.660 | 0.715 | 0.640 | 0.683 | 0.810 |
| Garden | 0.658 | 0.650 | 0.680 | 0.666 | 0.664 | 0.706 | 0.699 |
| Uncultivated | 0.620 | 0.652 | 0.663 | 0.685 | 0.670 | 0.692 | 0.721 |
| Meadow | 0.600 | 0.585 | 0.634 | 0.693 | 0.663 | 0.606 | 0.645 |
| Arable land | 0.622 | 0.719 | 0.653 | 0.702 | 0.656 | 0.757 | 0.877 |
| Olive grove | 0.855 | 0.699 | 0.608 | 0.699 | 0.685 | 0.650 | |
| Vineyard | 0.581 | 0.692 | 0.659 | 0.706 | 0.699 | 0.640 | 0.752 |
| Shrubs | 0.630 | 0.707 | 0.730 | 0.846 | 0.670 | | 0.685 |
| Rocks | 0.638 | 0.710 | 0.638 | 0.511 | | | |

All the measured reliability values are greater than 0.5, indicating that, on average, the degree of membership in the Gaussian fuzzy set corresponding to the class to which a green

area belongs is a value greater than 0.5. This result shows that the uncertainty of assigning an urban green area to an NDVI, NDMI, and LST class can be considered negligible.

3.2. Discussion of the Results: An Analysis of the Behavior of the Types of Greenery

The results obtained for the different types of greenery are analyzed in detail below. For brevity, detailed results are presented for three types of greenery: for the predominantly broad-leaved forests and olive groves, which, like reeds and shrubs, were found to be less vulnerable during the heatwave, and for the uncultivated areas, which instead have shown more critical behaviors during this period.

As can be seen from the histograms in Figure 9, the predominantly broad-leaved forests are classified mostly with NDVI and NDMI classes of Medium high, High, and Very high (respectively, 81.82% and 85.17%); on the contrary, they are classified largely as having an LST class of Medium low and Very low (87.56%). Only 8% of the predominantly broad-leaved forests are classified with an NDVI of Medium Low and only 1% with an NDVI of Low. Similarly, only 12% are classified with an NDMI of Medium Low and only 2% with an NDMI of Low. From this it can be deduced that the health status of this type of urban greenery remained good during the heatwave. Furthermore, since only 5% of the forest areas are classified with an LST of Medium high and none of them are classified with an LST of High or Very high, it can be concluded that these types of urban greenery were able to cool the soil during the heatwave.

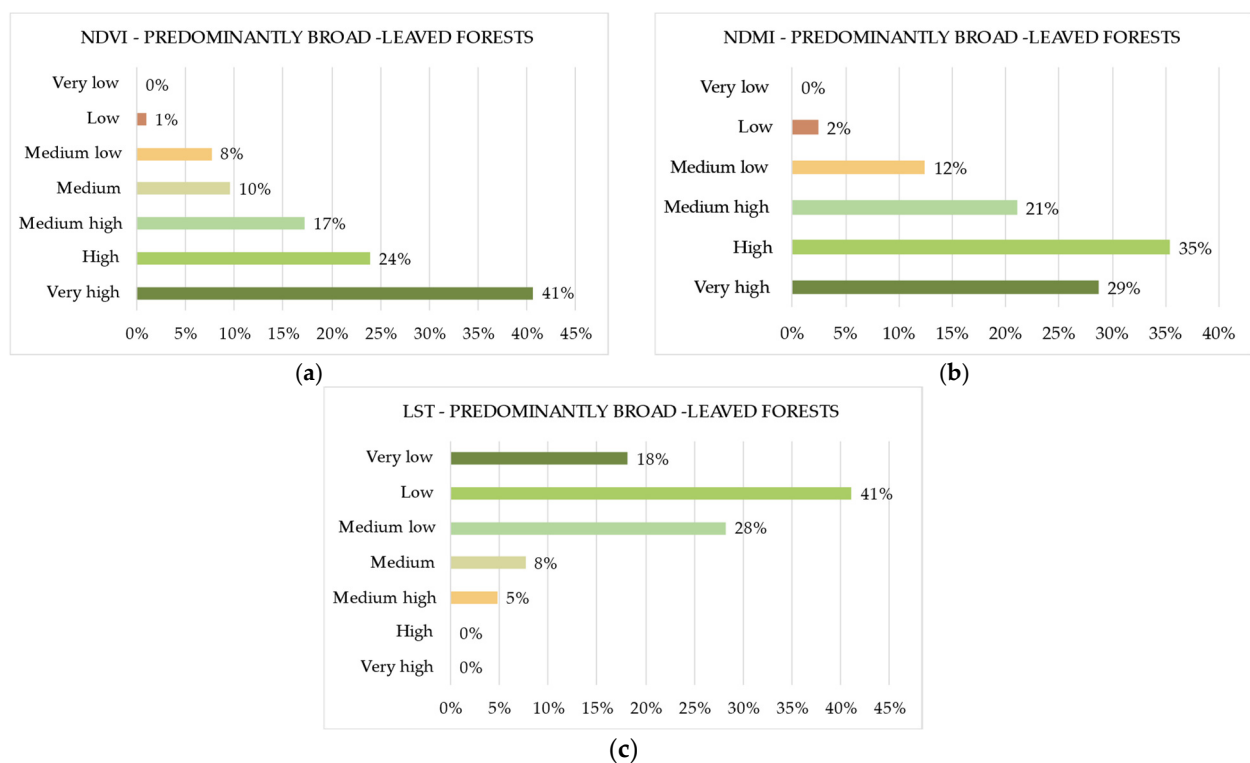


Figure 9. Frequency distribution of predominantly broad-leaved forests for the classes of each of the three indices of NDVI (a), NDMI (b), and LST (c).

These results denote that urban greenery composed of broad-leaved forests during heat waves maintains optimal levels of efficiency in terms of the presence of live vegetation, percentage of humidity, and temperatures that are not high on the ground.

Olive groves also show similar behavior to that of deciduous forest areas, with a prevalence of olive groves classified with NDVI and NDMI classes of Medium high, High, and Very high equal to, respectively, 63.90% and 83.39% (Figure 10a,b). Furthermore,

53.05% of the olive groves are mainly classified as having an LST of Low or Medium low (Figure 10c).

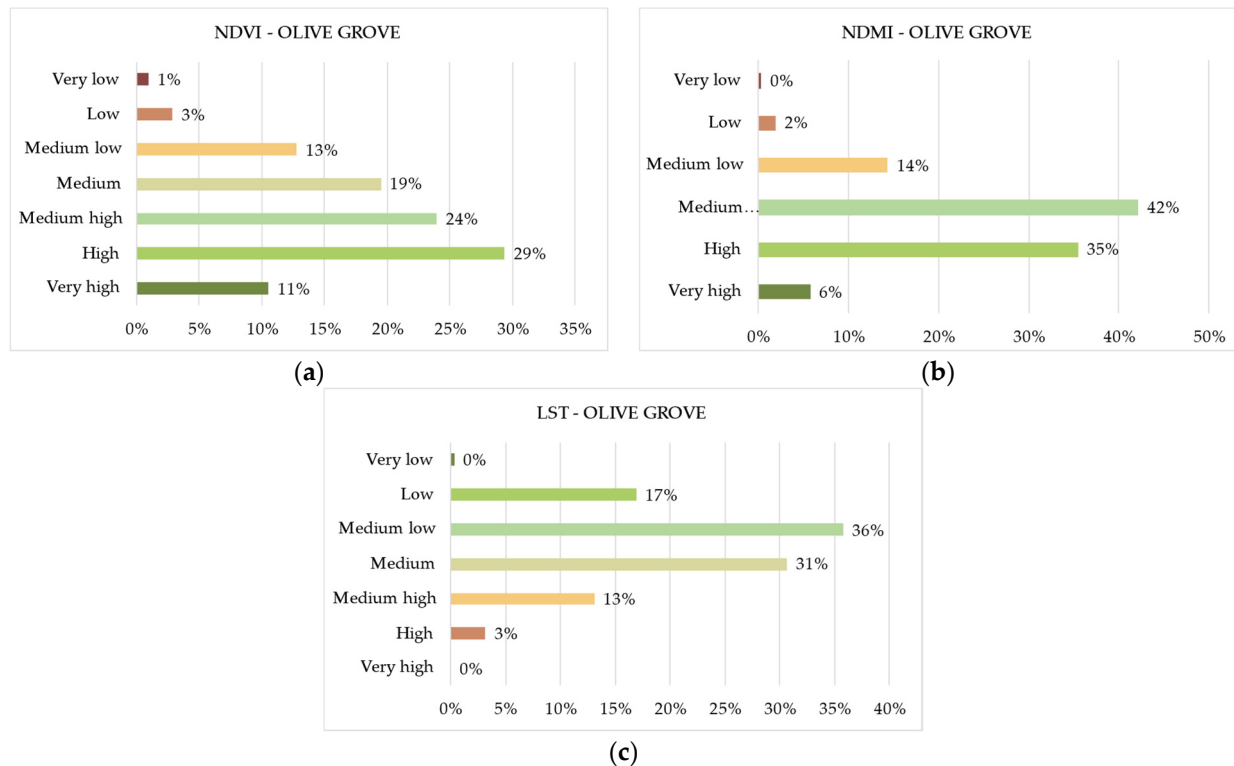


Figure 10. Frequency distribution of olive groves for the classes of each of the three indices of NDVI (a), NDMI (b), and LST (c).

In summary, olive groves showed, during the heatwave, the presence of live vegetation and good humidity, even if this was not as optimal as that of urban forest areas with a prevalence of broad-leaved trees. Furthermore, even olive groves were able to maintain an acceptable soil temperature during this period (only 13% of them were classified with an LST of Medium high and only 3% with an LST of High).

A different behavior is shown by uncultivated areas; they are classified mainly with an NDVI and NDMI of Medium low, Low, and Very low, with values of 42.28% and 51.77%, respectively (Figure 11a,b). Furthermore, they are mainly classified with an LST of Medium high, High, and Very high, with a value equal to 53.86%. Only 9% of uncultivated areas are classified with an LST of Low and Very low, while 54% of them are classified with an LST of at least Medium high (Figure 11c).

This trend highlights that uncultivated areas during heatwaves represent critical urban green areas, being devoid of living vegetation, predominantly arid, and with a reduced capacity to absorb or reduce thermal energy to the ground.

These results are in line with the findings obtained in [39], in which measurements recorded by in situ and mobile sensors around four urban areas were used to evaluate the cooling efficiency of green nature-based solutions.

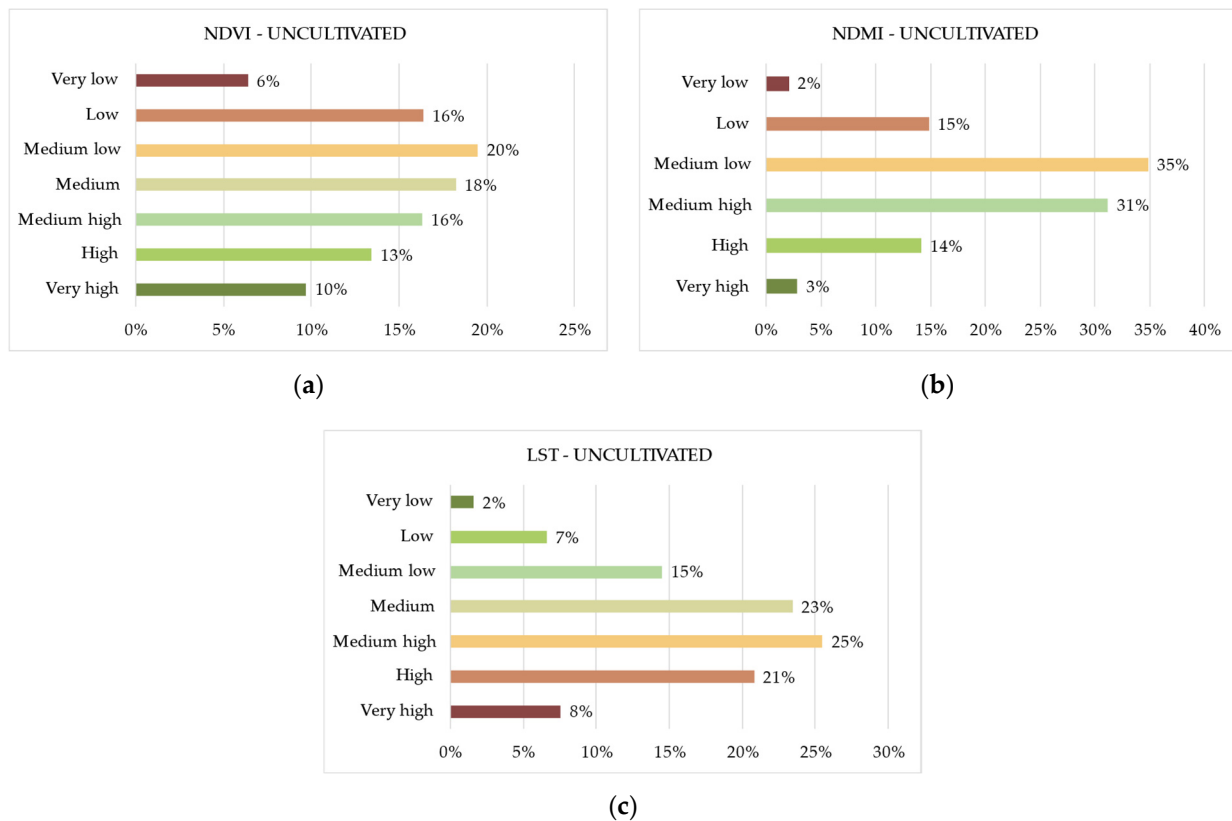


Figure 11. Frequency distribution of uncultivated areas for the classes of each of the three indices of NDVI (a), NDMI (b), and LST (c).

3.3. Study Limitations

The proposed method provides a comprehensive analysis of urban greenery behavior during heatwaves, without necessitating high spatial accuracy, as evidenced by these results. It has the advantage of being computationally fast and does not require data having high spatial resolution.

However, a more in-depth analysis including additional greenery characteristics requires measuring other vegetation parameters, such as leaf area index (LAI), enhanced vegetation index (EVI), soil adjusted vegetation index (SAVI), and gross primary productivity (GPP). Furthermore, corrections for atmospheric and soil disturbance effects must be applied to increase the spatial accuracy.

4. Conclusions

In this work, a GIS-based model was proposed to evaluate the behavior of urban greenery during heatwaves, by analyzing the distribution of NDVI, NDMI, and LST of green areas in the urban settlement under investigation.

The model uses an unsupervised classification method using NDVI, NDMI, and LST, which allows the optimization of the similarity between urban green areas belonging to a class and the dissimilarity between green areas in different classes. Furthermore, by assigning a Gaussian fuzzy set to each class, the model provides an assessment of the reliability of the assignment of urban greenery types to a class. The model was tested to analyze the behavior of types of urban greenery present in the city of Naples (Italy) during a period of heatwaves. The results highlighted that some types of urban greenery, such as forest areas with a prevalence of broad-leaved trees and olive groves, had optimal behavior over the period, recording, on average, high values of NDVI and NDMI, and, on average, low values of LST. On the contrary, uncultivated areas appear to have predominantly low values of NDVI and NDMI and predominantly high values of LST.

The proposed method has the advantage of being computationally fast and providing a picture of the health and cooling potential of urban greenery during heatwaves. It can represent valid decision support in the choices of adaptive transformation, and plant or maintenance actions to be carried out in urban settlements to deal with heatwave scenarios.

A critical point of this research is that further analyses in different urban contexts are needed in order to further validate the model and verify whether it is necessary to extend it by taking into account other vegetation indices and more accurate spatial resolutions.

We intend to carry out future research to improve the accuracy of the results, through the acquisition, at a more detailed scale, of the distribution of green urban areas and their characteristics, and by testing the model in different urban settlements and various heatwave scenarios.

Author Contributions: Conceptualization, Barbara Cardone, Ferdinando Di Martino, Cristiano Mauriello and Vittorio Miraglia; methodology, Barbara Cardone, Ferdinando Di Martino, Cristiano Mauriello and Vittorio Miraglia; software, Barbara Cardone, Ferdinando Di Martino, Cristiano Mauriello and Vittorio Miraglia; validation, Barbara Cardone, Ferdinando Di Martino, Cristiano Mauriello and Vittorio Miraglia; formal analysis, Barbara Cardone, Ferdinando Di Martino, Cristiano Mauriello and Vittorio Miraglia; investigation, Barbara Cardone, Ferdinando Di Martino, Cristiano Mauriello and Vittorio Miraglia; resources, Barbara Cardone, Ferdinando Di Martino, Cristiano Mauriello and Vittorio Miraglia; data curation, Barbara Cardone, Ferdinando Di Martino, Cristiano Mauriello and Vittorio Miraglia; writing—original draft preparation, Barbara Cardone, Ferdinando Di Martino, Cristiano Mauriello and Vittorio Miraglia; writing—review and editing, Barbara Cardone, Ferdinando Di Martino, Cristiano Mauriello and Vittorio Miraglia; visualization, Barbara Cardone, Ferdinando Di Martino, Cristiano Mauriello and Vittorio Miraglia; supervision, Barbara Cardone, Ferdinando Di Martino, Cristiano Mauriello and Vittorio Miraglia. All authors have read and agreed to the published version of the manuscript.

Funding: This research received no external funding.

Data Availability Statement: The data presented in this study are available on request from the corresponding author.

Conflicts of Interest: The authors declare no conflicts of interest.

References

1. Jedlovec, G.; Crane, D.; Quattrochi, D. Urban heat wave hazard and risk assessment. *Results Phys.* **2017**, *7*, 4294–4295. [[CrossRef](#)]
2. Cheval, S.; Dumitrescu, A.; Amihăesei, V.; Iraşoc, A.; Paraschiv, M.G.; Ghent, D. A country scale assessment of the heat hazard-risk in urban areas. *Buold. Environ.* **2023**, *229*, 109892. [[CrossRef](#)]
3. D’Ambrosio, V.; Di Martino, F.; Miraglia, V. A GIS-based framework to assess heatwave vulnerability and impact scenarios in urban systems. *Sci. Rep.* **2023**, *13*, 13073. [[CrossRef](#)] [[PubMed](#)]
4. Jaung, W.; Carrasco, L.R.; Shaikh, S.F.E.A.; Tan, P.Y.; Richards, D.R. Temperature and air pollution reductions by urban green spaces are highly valued in a tropical city-state. *Urban For. Urban Greenery* **2020**, *55*, 126827. [[CrossRef](#)]
5. Mabon, L.; Shih, W.Y. Urban greenspace as a climate change adaptation strategy for subtropical Asian cities: A comparative study across cities in three countries. *Glob. Environ. Change* **2021**, *68*, 102248. [[CrossRef](#)]
6. Kumar, P.; Debele, S.E.; Khalili, S.; Halios, C.H.; Sahani, J.; Aghamohammadi, N.; de Fatima Andrade, M.; Athanassiadou, M.; Bhui, K.; Calvillo, N.; et al. Urban heat mitigation by green and blue infrastructure: Drivers, effectiveness, and future needs. *Innovation* **2024**, *5*, 100588. [[CrossRef](#)]
7. Zhou, W.; Yu, M.; Zhang, Z.; Cao, W.; Wu, T. How can urban green spaces be planned to mitigate urban heat island effect under different climatic backgrounds? A threshold-based perspective. *Sci. Total Environ.* **2023**, *809*, 164422. [[CrossRef](#)]
8. Semenzato, P.; Bortolini, L. Urban Heat Island Mitigation and Urban Green Spaces: Testing a Model in the City of Padova (Italy). *Land* **2023**, *12*, 476. [[CrossRef](#)]
9. Li, W.; Sun, R. A supply-demand model of vegetation cooling for urban heatwave mitigation. *Urban Clim.* **2023**, *52*, 101699. [[CrossRef](#)]
10. Cafaro, R.; Cardone, B.; D’Ambrosio, V.; Di Martino, F.; Miraglia, V. A New GIS-Based Framework to Detect Urban Heat Islands and Its Application on the City of Naples (Italy). *Land* **2024**, *13*, 1253. [[CrossRef](#)]
11. Cardone, B.; D’Ambrosio, V.; Di Martino, F.; Miraglia, V.; Rigillo, M. Analysis of the Ecological Efficiency Increase of Urban Green Areas in Densely Populated Cities. *Land* **2023**, *12*, 523. [[CrossRef](#)]
12. Francini, M.; Salvo, C.; Vitale, A. Combining Deep Learning and Multi-Source GIS Methods to Analyze Urban and Greening Changes. *Sensors* **2023**, *23*, 3805. [[CrossRef](#)] [[PubMed](#)]

13. Stessens, P.; Canters, F.; Huysmans, M.; Khan, A.Z. Urban green space qualities: An integrated approach towards GIS-based assessment reflecting user perception. *Land Use Policy* **2020**, *91*, 104319. [[CrossRef](#)]
14. Cardone, B.; Cerreta, M.; Di Martino, F.; Miraglia, V.; Sacco, S. A fuzzy-based emotion detection method to classify the attractiveness of urban green space. *Evol. Intell.* **2024**, *17*, 3921–3933. [[CrossRef](#)]
15. Shahtahmassebi, A.R.; Li, C.; Fan, Y.; Wu, Y.; Lin, Y.; Gan, M.; Wang, K.; Malik, A.; Blackburn, G.A. Remote sensing of urban green spaces: A review. *Urban For. Urban Green.* **2021**, *57*, 126946. [[CrossRef](#)]
16. Zahir, I.L.M.; Nuskiya, M.H.F.; Sangasumana, V.P.; Iyoob, A.L.; Ameer, M.L.F. Monitoring Urban Green Space Using Remote Sensing Derived-vegetation Indices in Colombo District, Sri Lanka. *Procedia Comput. Sci.* **2024**, *236*, 248–256. [[CrossRef](#)]
17. Serrano, J.; Shahidian, S.; Marques da Silva, J. Evaluation of normalized difference water index as a tool for monitoring pasture seasonal and inter-annual variability in a mediterranean agro-silvo-pastoral system. *Water* **2019**, *11*, 62. [[CrossRef](#)]
18. Dutta, D.; Rahman, A.; Paul, S.K.; Kundu, A. Spatial and temporal trends of urban green spaces: An assessment using hyper-temporal NDVI datasets. *Geocarto Int.* **2022**, *37*, 7983–8003. [[CrossRef](#)]
19. de la Iglesia Martinez, A.; Labib, S.M. Demystifying normalized difference vegetation index (NDVI) for greenness exposure assessments and policy interventions in urban greening. *Environ. Res.* **2023**, *220*, 115155. [[CrossRef](#)]
20. Aryal, J.; Sitaula, C.; Aryal, S. NDVI Threshold-Based Urban Green Space Mapping from Sentinel-2A at the Local Governmental Area (LGA) Level of Victoria, Australia. *Land* **2022**, *11*, 351. [[CrossRef](#)]
21. Strashok, O.; Ziemiańska, M.; Strashok, V. Evaluation and Correlation of Normalized Vegetation Index and Moisture Index in Kyiv (2017–2021). *J. Ecol. Eng.* **2022**, *23*, 212–218. [[CrossRef](#)]
22. Liu, Y.; Li, H.; Li, C.; Zhong, C.; Chen, X. An Investigation on Shenzhen Urban Green Space Changes and Their Effect on Local Eco-Environment in Recent Decades. *Sustainability* **2021**, *13*, 12549. [[CrossRef](#)]
23. Stumpe, B.; Bechtel, B.; Heil, J.; Jörges, C.; Jostmeier, A.; Kalks, F.; Schwarz, K.; Marschner, B. Soil texture mediates the surface cooling effect of urban and peri-urban green spaces during a drought period in the city area of Hamburg (Germany). *Sci. Total Environ.* **2023**, *897*, 165228. [[CrossRef](#)] [[PubMed](#)]
24. Shi, F.; Yang, B.; Li, M. An improved framework for assessing the impact of different urban development strategies on land cover and ecological quality changes—A case study from Nanjing Jiangbei New Area, China. *Ecol. Indic.* **2023**, *147*, 109998. [[CrossRef](#)]
25. Kim, J.; Khouakhi, A.; Corstanje, R.; Johnston, A.S.A. Greater local cooling effects of trees across globally distributed urban green spaces. *Sci. Total Environ.* **2024**, *911*, 168494. [[CrossRef](#)]
26. Sharma, R.; Joshi, P. K Identifying seasonal heat islands in urban settings of Delhi (India) using remotely sensed data—An anomaly-based approach. *Urban Clim.* **2014**, *9*, 19–34. [[CrossRef](#)]
27. Mukherjee, S.; Joshi, P.K.; Garg, R.D. Analysis of urban built-up areas and surface urban heat island using downscaled MODIS derived land surface temperature data. *Geocarto Int.* **2016**, *32*, 900–918. [[CrossRef](#)]
28. Kumar, S.; Panwar, M. Urban heat island footprint mapping of Delhi using remote sensing. *Int. J. Emerg. Technol.* **2017**, *8*, 80–83.
29. Renard, F.; Alonso, L.; Fitts, Y.; Hadjiiosif, A.; Comby, J. Evaluation of the Effect of Urban Redevelopment on Surface Urban Heat Islands. *Remote Sens.* **2019**, *11*, 299. [[CrossRef](#)]
30. Sarif, M.O.; Rimal, B.; Stork, N.E. Assessment of Changes in Land Use/Land Cover and Land Surface Temperatures and Their Impact on Surface Urban Heat Island Phenomena in the Kathmandu Valley (1988–2018). *ISPRS Int. J. Geo-Inf.* **2020**, *9*, 726. [[CrossRef](#)]
31. Nahin, K.T.K.; Sara, H.H.; Barai, K.R.; Quayyum, Z.; Baumgartner, J. Spatiotemporal Variability of Urban Greenspace and Surface Temperature in Dhaka City: A Public Health Aspect. In *The Empathic City. S.M.A.R.T. Environments*; Biloría, N., Sebag, G., Robertson, H., Eds.; Springer: Berlin/Heidelberg, Germany, 2023; pp. 143–170. [[CrossRef](#)]
32. Jenks, G.F. A Geographic Logic In Line Generalization. *Cartographica* **1989**, *26*, 27–42. [[CrossRef](#)]
33. Jenks, G.F. The Data Model Concept in Statistical Mapping. *Int. Yearb. Cartogr.* **1967**, *7*, 186–190.
34. North, M.A. A Method for Implementing a Statistically Significant Number of Data Classes in the Jenks Algorithm. In Proceedings of the 2009 Sixth International Conference on Fuzzy Systems and Knowledge Discovery, Tianjin, China, 14–16 August 2009; pp. 35–38. [[CrossRef](#)]
35. Du, C.; Ren, H.; Qin, Q.; Meng, J.; Zhao, S. A Practical Split-Window Algorithm for Estimating Land Surface Temperature from Landsat 8 Data. *Remote Sens.* **2015**, *7*, 647–665. [[CrossRef](#)]
36. Mohamed, M. Analysis of Digital Elevation Model and LANDSAT Data Using Geographic Information System for Soil Mapping in Urban Areas. *Nat. Resour.* **2017**, *8*, 767–787. [[CrossRef](#)]
37. Arbelaitz, O.; Gurrutxaga, I.; Muguerza, J.; Perez, J.M.; Perona, I. An extensive comparative study of cluster validity indices. *Pattern Recognit.* **2013**, *46*, 243–256. [[CrossRef](#)]
38. Schubert, E. Stop using the elbow criterion for k-means and how to choose the number of clusters instead. *ACM SIGKDD Explor. Newsl.* **2023**, *25*, 36–42. [[CrossRef](#)]
39. Sahani, J.; Kumar, P.; Debele, S.E. Efficacy assessment of green-blue nature-based solutions against environmental heat mitigation. *Environ. Int.* **2023**, *179*, 108187. [[CrossRef](#)]

Disclaimer/Publisher’s Note: The statements, opinions and data contained in all publications are solely those of the individual author(s) and contributor(s) and not of MDPI and/or the editor(s). MDPI and/or the editor(s) disclaim responsibility for any injury to people or property resulting from any ideas, methods, instructions or products referred to in the content.